Functional analysis of keratinocyte and fibroblast gene expression in skin and keloid scar tissue based on deviation analysis of dynamic capabilities

MINGMING LI[1] and LEI WU[2]

[1]Department of Cosmetology, Luoyang Central Hospital Affiliated to Zhengzhou University, Luoyang, Henan 471000; [2]Department of Plastic Surgery, The No. 1 People's Hospital of Zhengzhou, Zhengzhou, Henan 450003, P.R. China

Received July 3, 2015; Accepted September 1, 2016

DOI: 10.3892/etm.2016.3817

Abstract. The aim of the present study was to select key genes that are associated with fibroblasts and keratinocytes during keloid scar progression and development. The gene expression profile of GSE44270, which includes 32 samples, was downloaded from the Gene Expression Omnibus database. Differentially expressed genes (DEGs) in case samples compared with control samples were screened using the Limma R package followed by hierarchical clustering analysis. Protein-protein interaction (PPI) networks of the total selected DEGs were constructed using Cytoscape. Moreover, the Gene Ontology biological processes and significant Kyoto Encyclopedia of Genes and Genomes pathways of the total selected DEGs were enriched using the Database for Annotation, Visualization and Integrated Discovery. Significant pathways that may be associated with keloid scar were analyzed using deviation analysis of dynamic capabilities. There were 658 DEGs in fibroblast keloid vs. normal, 112 DEGs in fibroblast non-lesion vs. normal, 439 DEGs in fibroblast keloid vs. non-lesion, 523 DEGs in keratocyte keloid vs. normal, 186 DEGs in keratocyte non-lesion vs. normal, and 963 DEGs in keratocyte keloid vs. non-lesion groups. HOXA9, BMP4, CDKN1A and SMAD2 in fibroblasts, and HOXA7, MCM8, PSMA4 and PSMB2 in keratinocytes were key genes in the PPI networks. Moreover, the amino sugar and nucleotide sugar metabolism pathway, cell cycle, and extracellular matrix (ECM)-receptor interaction pathway were significant pathways. This study suggests that several key genes (BMP4, HOXA9, SMAD2, CDKN1A, HOXA7, PSMA4 and PSMB2) that participate in some significant pathways (cell cycle and ECM-receptor interaction pathways) may be potential therapeutic targets for keloid scars.

Correspondence to: Dr Mingming Li, Department of Cosmetology, Luoyang Central Hospital Affiliated to Zhengzhou University, 288 Middle Zhongzhou Road, Luoyang, Henan 471000, P.R. China
E-mail: mingminglidr@163.com

Key words: skin and keloid scar tissue, keratinocyte, fibroblast, differentially expressed genes, deviation analysis of dynamic capabilities

Introduction

Keloid scar of skin is a soft tissue benign skin tumor that originates from the proliferation of connective tissue following skin injury (1). Data show that the morbidity of keloid scars has been high in recent years, and female cases are more common than male cases (2). There are a variety of clinical treatment methods for keloids, including glucocorticoid injection under the skin, freezing, compression, ultrashort wave therapy, and simple surgery (3,4). However, clinical data reveal that the therapeutic effects are poor due to easy recurrence and high morbidity (5). Therefore, it is necessary to explore some biomarkers for keloid scar therapy in clinical practice.

The pathogenesis of keloid scar formation is complicated, particularly the key roles of fibroblasts and keratinocytes in this type of disease (6,7). Werner *et al* demonstrated that keratinocytes interact with fibroblasts and then function in wound healing (8). Keloid-derived keratinocytes were shown to perform a promoting role on fibroblast growth and proliferation in an *in vitro* study (7). Furthermore, there is increasing evidence that many key molecules play crucial roles during keloid scar development through fibroblasts and keratinocytes from a molecular perspective. For instance, downregulation of the inhibitors SMAD6 and SMAD7 was found in keloid scar tissue (9), and overexpression of bone morphogenetic protein (BMP)2 contributed to fibroblast cell proliferation and collagen synthesis during cholesteatoma progression (10). Although many researchers have focused on the pathogenesis of fibroblasts and keratinocytes in keloid scar development and progression, the molecular mechanism remains incompletely elucidated.

Gene expression analysis provides the basis for predicting target genes that are associated with many diseases. Hahn *et al* investigated abnormally expressed genes in keloid keratinocytes and fibroblasts using the GSE44270 microarray (11). In the present study, the expression of functional genes of keloid keratinocytes and fibroblasts was analyzed using the same gene expression profile. Comprehensive bioinformatics methods were used to analyze the significant biological processes and

pathways of differentially expressed genes (DEGs) that are associated with the pathogenesis of keloids. This study aimed to identify several key genes and investigate the key pathways that are associated with the development and progression of keloid scarring of skin.

Materials and methods

Data resources and data preprocessing. The gene expression profile of GSE44270, which includes 32 samples, was downloaded from the National Center of Biotechnology Information (NCBI) Gene Expression Omnibus database (http://www.ncbi.nlm.nih.gov/geo/) based on the platform [HuGene-1_0-st] Affymetrix Human Gene 1.0 ST Array [transcript (gene) version] (Affymetrix, Inc., Santa Clara, CA, USA). The data contains 3 control fibroblast, 3 control keratinocyte, 9 keloid fibroblast, 9 keloid keratinocyte, 4 non-lesional fibroblast and 4 non-keratinocyte samples. Skin and scar tissues were collected for the isolation of primary keratinocytes and fibroblasts, and keloid scars were excised from patients undergoing elective plastic surgery. Control samples were from normal skin tissues. The total samples were separated into six groups, specifically, fibroblast keloid vs. normal, fibroblast non-lesion vs. normal, fibroblast keloid vs. non-lesion, keratocyte keloid vs. normal, keratocyte non-lesion vs. normal, and keratocyte keloid vs. non-lesion.

The downloaded files were preprocessed using the R package in the Robust Multi-array Analysis (RMA) method (12). The probe IDs were transformed into gene bank IDs using Database for Annotation, Visualization and Integrated Discovery (DAVID) software (13).

DEG screening. The DEGs in case samples compared with the control samples were screened using the R package in Limma (14). An adjusted P-value based on false discovery rate (FDR) of <0.01 (15) and $\log_2$ |fold change (FC)| >1 were chosen as the thresholds.

Hierarchical clustering analysis of DEGs. In order to identify the selected DEGs from different tissue samples, hierarchical clustering was used to analyze the total selected DEGs from the fibroblast or keratinocyte samples using the Python programming language (16). Also, Pearson correlation was used to establish the similarity matrix of DEGs (17), and the type of linkage used was the average linkage (18).

Protein-protein interaction (PPI) network construction. In order to investigate the potential genes that interacted with the selected DEGs, the total screened DEGs were used to construct a PPI network based on the BioGRID database (19) and the Human Protein Reference Database (HPRD) database (20). Cytoscape (21) was used to conduct a topological analysis of the constructed network to study the node degrees of the DEGs.

Functional enrichment analysis of the DEGs. The biological processes and significant pathways for the total selected DEGs in the six groups were enriched using the DAVID online software with (Gene Ontology) GO and Kyoto Encyclopedia of Genes and Genomes (KEGG) terms. Terms with DEG number >10 and P<0.05 were selected as they were considered to be significant terms.

Deviation analysis of dynamic capabilities. The enriched biological processes and pathways of DEGs in the three groups (non-lesion vs. normal, keloid vs. normal and keloid vs. non-lesion) suggested some significant pathways that were involved in the process of skin and scar pathogenesis from normal to non-lesion, and then to skin and scar disease. The dynamic capability of each significant pathway term was calculated with the following formula (22):

$$A(P) = \frac{1}{N}\sum_{i=1}^{N}\sqrt{\omega(X_i - Y_i)^2}$$

P represents function, A(P) represents the deviation score, N represents the number of DEGs, X_i represents the average expression value for one DEG i in disease development, Yi represents the average gene expression value for one gene i in normal tissues, and ω represents the node degree for DEG i in the PPI network. Euclidean distances of the total DEGs between case samples and normal samples were calculated to predict the deviation degree of DEGs in case samples (non-lesion or keratocyte keloid) compared with the normal samples.

Results

DEG screening and hierarchical clustering analysis. The total DEGs in the six groups were selected using the Limma package with an adjusted P-value <0.01 and $\log_2$|FC| >1 compared with the control samples (Table I). There were 658 DEGs in the fibroblast keloid vs. normal group, 112 DEGs in the fibroblast non-lesion vs. normal group, 439 DEGs in the fibroblast keloid vs. non-lesion group, 523 DEGs in the keratocyte keloid vs. normal group, 186 DEGs in the keratocyte non-lesion vs. normal group, and 963 DEGs in the keratocyte keloid vs. non-lesion group. A Venn plot of the total screened DEGs is shown in Fig. 1A; there were 2 common DEGs in keratinocytes and 1 common DEG in fibroblasts during the progression of skin and scar pathogenesis. In addition, the hierarchical clustering of the DEGs in each group is shown in Fig. 1B.

PPI network construction. The screened DEGs in the different groups were used to construct the PPI network. The results showed that there were a total of 456 nodes (83 upregulated, 92 downregulated and 281 other DEGs obtained between lesion and non-lesion tissues) in the PPI network of DEGs in keratinocytes (Fig. 2), and there were a total of 374 nodes (74 upregulated, 181 downregulated, and 119 other DEGs obtained between lesion and non-lesion tissues) in the PPI network of DEGs in fibroblasts (Fig. 3). The results showed that DEGs such as homeobox A9 (HOXA9), BMP4, and phosphoinositide-3-kinase, regulatory subunit 1 α (PIK3R1) were upregulated while cyclin-dependent kinase inhibitor 1A (p21, Cip1) (CDKN1A), and SMAD family member 2 (SMAD2) were downregulated in fibroblasts. Also, DEGs including HOXA7, minichromosome maintenance complex component 8 (MCM8), and GRB2-associated binding protein 1 (GAB1) were upregulated while proteasome (prosome, macropain) subunit, α type, 4 (PSMA4), PSMB2, and cyclin-dependent kinase 1 (CDK1) were

Table I. Differentially expressed genes in each group.

Groups	Upregulated	Downregulated	Total
Fibroblast keloid vs. normal	196	462	658
Fibroblast non-lesion vs. normal	73	39	112
Fibroblast keloid vs. non-lesion	76	363	439
Keratocyte keloid vs. normal	224	299	523
Keratocyte non-lesion vs. normal	108	78	186
Keratocyte keloid vs. nonlesion	139	824	963

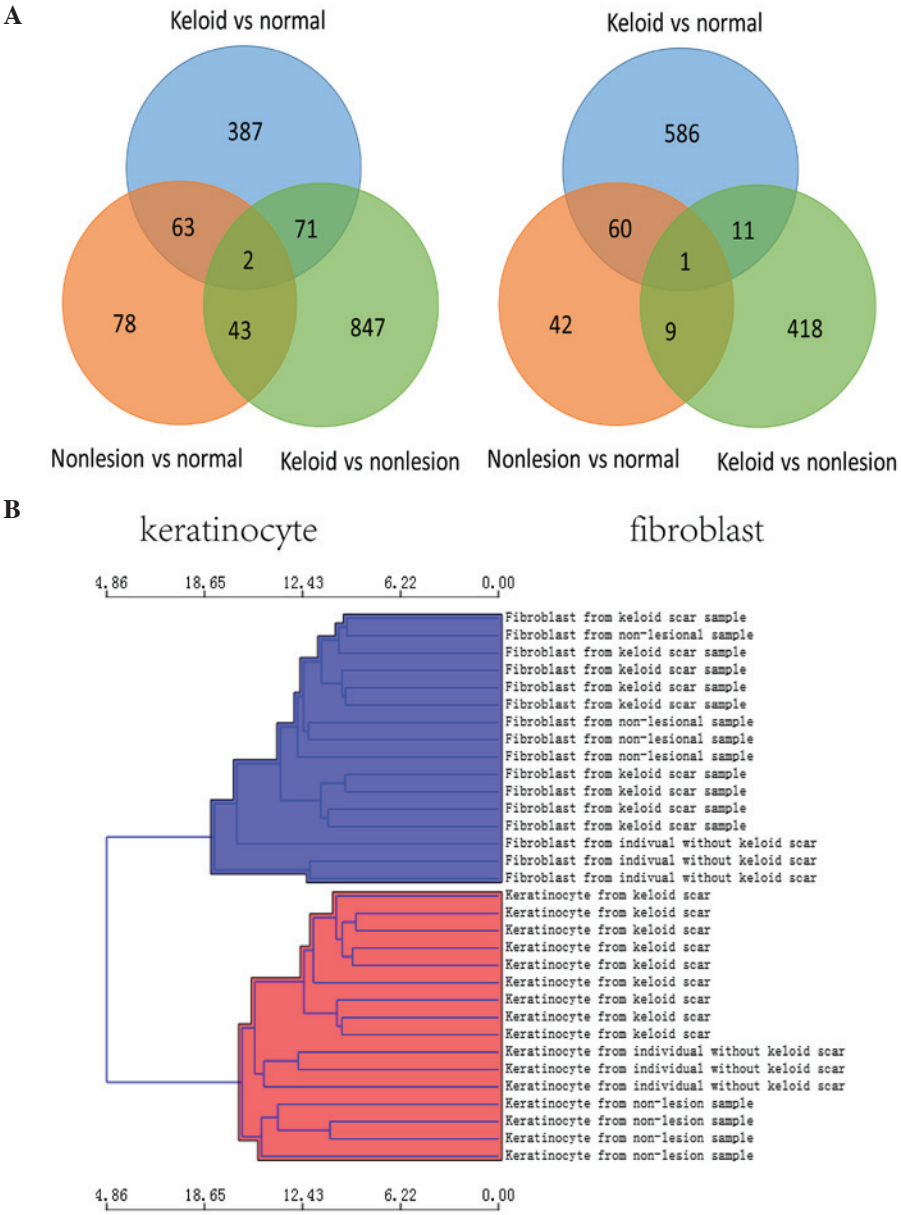

Figure 1. Analysis of the total screened differentially expressed genes (DEGs) in each group. (A) Venn plot of DEGs in each group from the two types of cell; (B) hierarchical clustering analysis between DEGs and samples. Samples are listed from the top to bottom.

downregulated in keratinocytes. In addition, structure specific recognition protein 1 (SSRP1) was a common gene in both keratinocytes and fibroblasts; however, it was only upregulated in fibroblast samples.

Functional enrichment analysis of the DEGs in each group. The significant biological processes and pathways of screened DEGs in fibroblast and keratinocyte groups were analyzed (Table II). The results revealed that DEGs in fibroblast samples

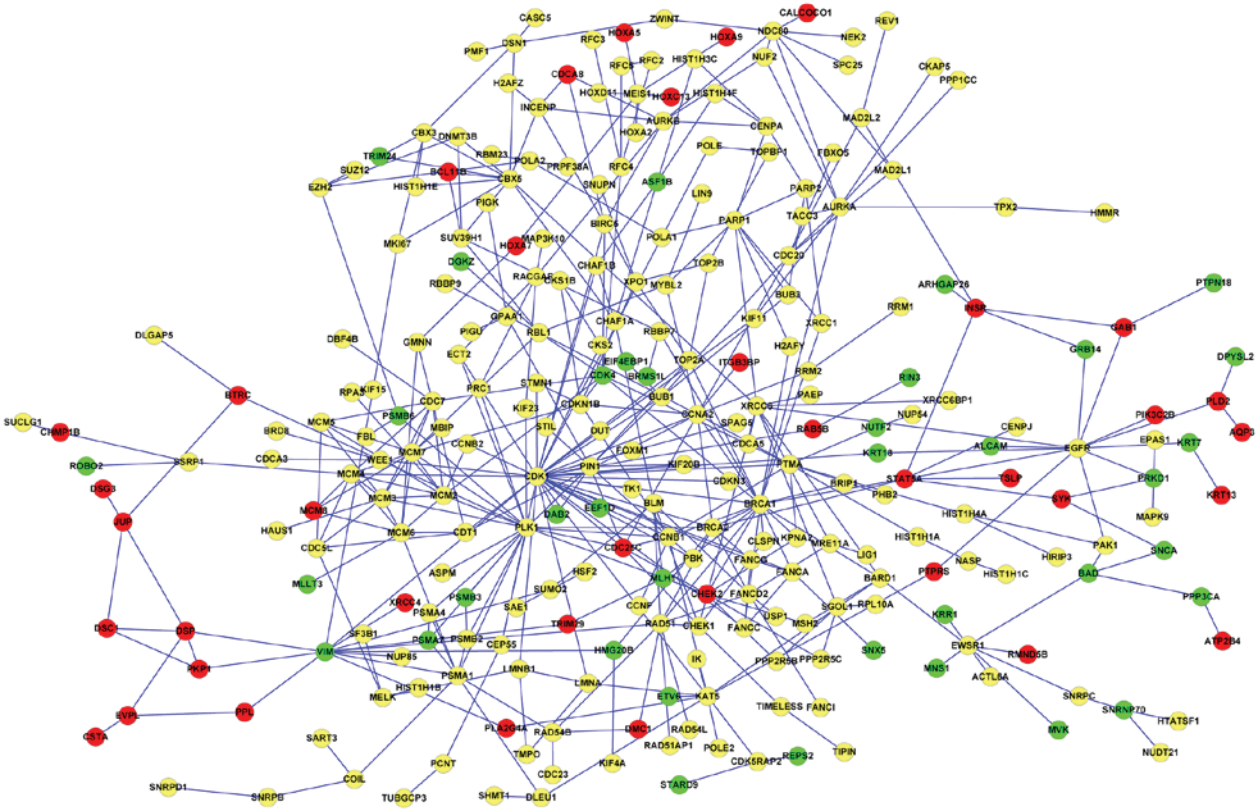

Figure 2. Protein-protein interaction (PPI) network of differentially expressed genes (DEGs) in keratinocytes. Green nodes represent downregulated DEGs compared with normal tissues, red nodes represent upregulated DEGs compared with normal tissues, and yellow nodes represent other interacting genes.

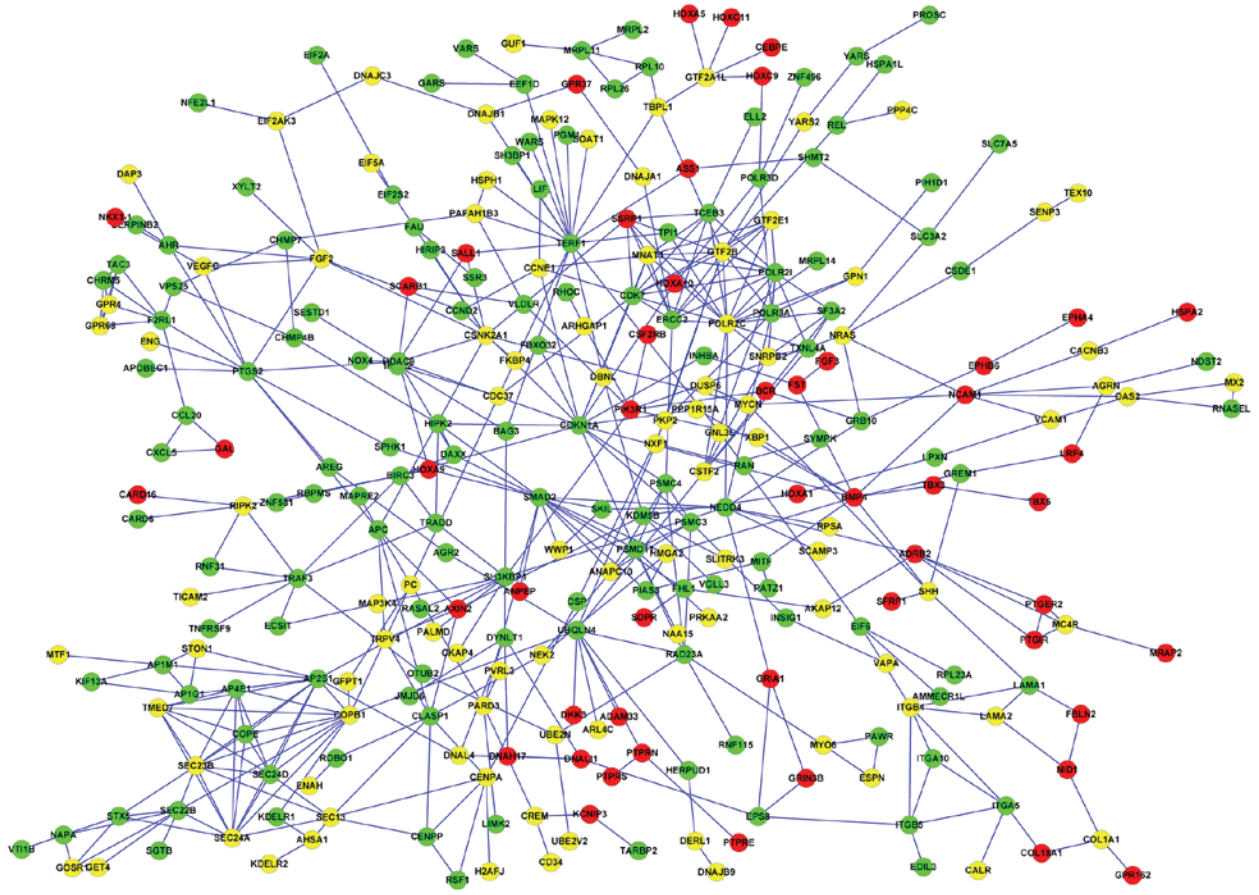

Figure 3. Protein-protein interaction (PPI) network of differentially expressed genes (DEGs) in fibroblasts. Green nodes represent down-regulated DEGs compared with normal tissues, red nodes represent upregulated DEGs compared with normal tissues, and yellow nodes represent other interacting genes.

Table II. Enrichment analysis of DEGs in different groups.

A, Enriched GO terms of DEGs

Term	Description	Count	P-value
Fibroblast tissues			
GO:0009952	Anterior/posterior pattern formation	24	7.39E-07
GO:0048706	Embryonic skeletal system development	17	1.53E-06
GO:0048704	Embryonic skeletal system morphogenesis	12	1.34E-04
GO:0043009	Chordate embryonic development	32	9.87E-04
GO:0009887	Organ morphogenesis	47	0.001376399
GO:0048705	Skeletal system morphogenesis	15	0.001849598
GO:0048193	Golgi vesicle transport	16	0.003092941
GO:0031327	Negative regulation of cellular biosynthetic process	44	0.006042035
GO:0010558	Negative regulation of macromolecule biosynthetic process	43	0.0064047
GO:0010629	Negative regulation of gene expression	40	0.007441896
GO:0009890	Negative regulation of biosynthetic process	44	0.008715561
GO:0045934	Negative regulation of nucleobase metabolic process	40	0.009747494
Keratinocyte tissues			
GO:0000279	M phase	117	9.33E-49
GO:0000087	M phase of mitotic cell cycle	89	2.37E-41
GO:0007067	Mitosis	88	3.71E-41
GO:0006259	DNA metabolic process	114	6.55E-27
GO:0006260	DNA replication	64	4.87E-25
GO:0006281	DNA repair	69	3.25E-18
GO:0007051	Spindle organization	23	1.37E-13
GO:0000070	Mitotic sister chromatid segregation	20	1.09E-12
GO:0010564	Regulation of cell cycle process	34	8.10E-12
GO:0065004	Protein-DNA complex assembly	29	6.32E-11

B, Enriched KEGG pathways of DEGs

Term	Pathway	Count	P-value
Fibroblast tissues			
hsa00520	Amino sugar and nucleotide sugar metabolism	10	3.92E-04
hsa00532	Chondroitin sulfate biosynthesis	5	0.02634733
hsa00330	Arginine and proline metabolism	7	0.02922789
hsa00970	Aminoacyl-tRNA biosynthesis	6	0.03313658
hsa05222	Small cell lung cancer	9	0.03478867
hsa04512	ECM-receptor interaction	9	0.04478867
Keratinocyte tissues			
hsa03030	DNA replication	23	1.19E-16
hsa04110	Cell cycle	34	4.86E-11
hsa03430	Mismatch repair	10	2.06E-05
hsa03040	Spliceosome	24	4.27E-05
hsa04114	Oocyte meiosis	22	4.63E-05
hsa03440	Homologous recombination	10	1.24E-04
hsa03410	Base excision repair	11	1.59E-04
hsa03420	Nucleotide excision repair	11	0.001171
hsa00240	Pyrimidine metabolism	16	0.004088
hsa00230	Purine metabolism	21	0.009136

DEGs, differentially expressed genes; GO, Gene Ontology; KEGG, Kyoto Encyclopedia of Genes and Genomes; ECM, extracellular matrix.

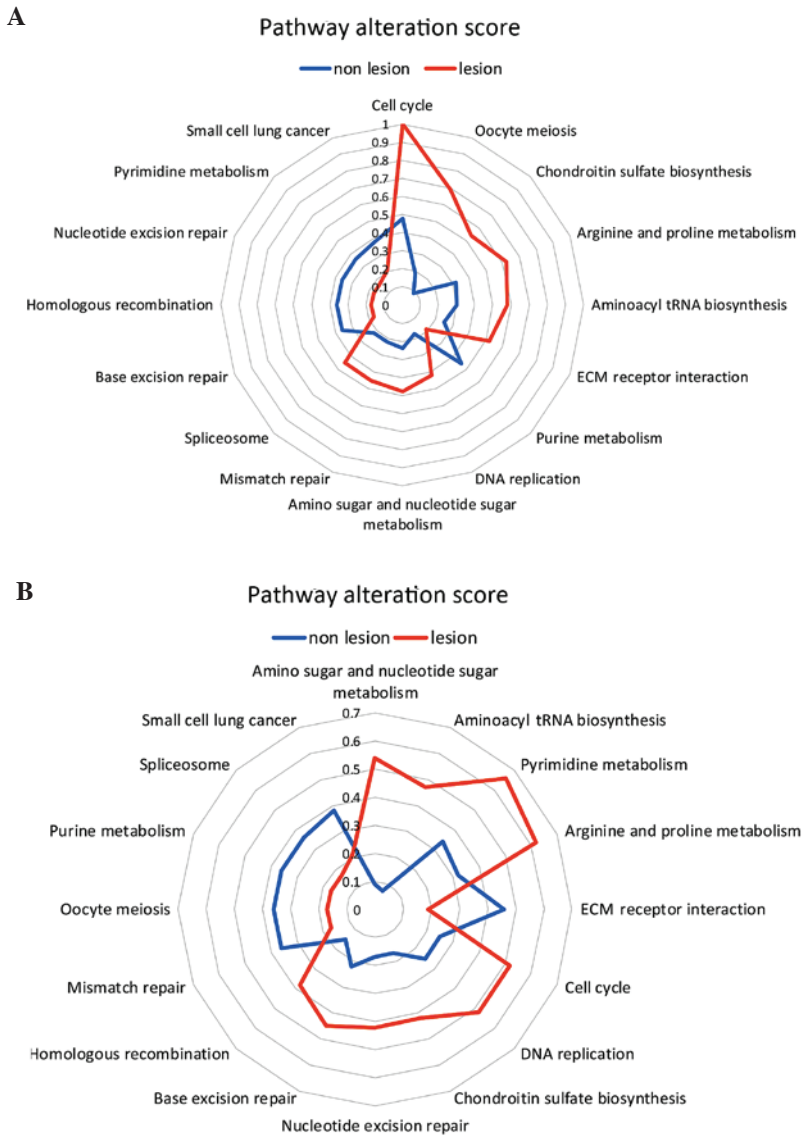

Figure 4. Pathway alteration scores of differentially expressed genes (DEGs) in each group. Pathway alteration scores of DEGs in (A) fibroblast samples and (B) keratinocyte samples. A score ~0 represents a function closely similar to that in the normal group, while the further a score is from the center of the circle the greater the apparent deviation of dynamic capability.

were enriched in significant GO terms such as negative regulation of cellular biosynthetic process, organ morphogenesis, and chordate embryonic development (Table IIA), and the total DEGs were involved in significant pathways such as the amino sugar and nucleotide sugar metabolism pathway and the extracellular matrix (ECM)-receptor interaction pathway (Table IIB). In addition, DEGs in keratinocyte samples were enriched in significant GO terms such as M phase, DNA metabolic process, and M phase of mitotic cell cycle (Table IIA), and the DEGs participated in the significant pathways of spliceosome, cell cycle, and DNA replication (Table IIB).

Deviation analysis of dynamic capabilities. A total of 16 pathways of DEGs from the fibroblast and keratinocyte groups were analyzed for deviation of dynamic capabilities (Fig. 4). Scores of pathways such as chondroitin sulfate biosynthesis (0.09) and oocyte meiosis (0.19) in the non-lesion group, and base excision repair (0.17), homologous recombination (0.17), and pyrimidine metabolism (0.17) in the lesion group indicated that DEGs involved in these pathways were similar to those in normal tissues (Table III). Furthermore, amino sugar and nucleotide sugar metabolism (0.09) and aminoacyl tRNA biosynthesis (0.07) in the non-lesion group, and base excision repair (0.17), homologous recombination (0.17), and pyrimidine metabolism (0.17) in the lesion group suggested that DEGs involved in these pathways were similar to those of DEGs in normal tissues (Table III).

Discussion

Keloid scar of skin is a type of benign soft tissue skin tumor that originates from the proliferation of connective tissue subsequent to skin injury, and has high morbidity (1,2). The identification of some clinical biomarkers for keloid scars would be of great significance. In the present study, the gene expression profile of GSE44270 was analyzed to screen

Table III. Pathway alteration scores of DEGs in different groups.

Pathway	Score of the enriched pathways of DEGs		
	Non-lesion	Lesion	Distance
Fibroblasts			
Cell cycle	0.48	1	0.52
Oocyte meiosis	0.19	0.69	0.5
Chondroitin sulfate biosynthesis	0.09	0.54	0.45
Arginine and proline metabolism	0.32	0.62	0.3
Aminoacyl tRNA biosynthesis	0.3	0.58	0.28
ECM-receptor interaction	0.25	0.52	0.27
Purine metabolism	0.46	0.19	0.27
DNA replication	0.17	0.42	0.25
Amino sugar and nucleotide sugar metabolism	0.24	0.48	0.24
Mismatch repair	0.22	0.45	0.23
Spliceosome	0.22	0.45	0.23
Base excision repair	0.36	0.17	0.19
Homologous recombination	0.36	0.17	0.19
Nucleotide excision repair	0.36	0.17	0.19
Pyrimidine metabolism	0.36	0.17	0.19
Small cell lung cancer	0.38	0.21	0.17
Keratinocytes			
Amino sugar and nucleotide sugar metabolism	0.09	0.54	0.45
Aminoacyl tRNA biosynthesis	0.07	0.47	0.4
Pyrimidine metabolism	0.34	0.66	0.32
Arginine and proline metabolism	0.32	0.62	0.3
ECM-receptor interaction	0.46	0.19	0.27
Cell cycle	0.25	0.52	0.27
DNA replication	0.25	0.52	0.27
Chondroitin sulfate biosynthesis	0.17	0.42	0.25
Nucleotide excision repair	0.17	0.42	0.25
Base excision repair	0.22	0.45	0.23
Homologous recombination	0.15	0.38	0.23
Mismatch repair	0.36	0.17	0.19
Oocyte meiosis	0.36	0.17	0.19
Purine metabolism	0.36	0.17	0.19
Spliceosome	0.36	0.17	0.19
Small cell lung cancer	0.38	0.21	0.17

DEGs, differentially expressed genes; ECM, extracellular matrix.

several key genes for skin and keloid scars and investigate the mechanisms involving fibroblasts and keratinocytes in keloid scar progression. The results demonstrated that many key genes that are involved in several significant pathways are crucial for keloid scars.

The present data indicated that BMP4 and HOXA9 are upregulated, and SMAD2 and CDKN1A are downregulated during the development and progression in fibroblasts. BMP4 is a protein of the bone morphogenetic family that belongs to the transforming growth factor superfamily, and is reported to play crucial roles in fibroblast proliferation (23), and an imbalance between proliferation and apoptotic cells in fibroblasts has been shown to be associated with keloids (24). Russell *et al* demonstrated that decreased expression of HOXA9 was correlated with wound healing in keloid-derived fibroblasts (25). Thus, overexpression of HOXA9 and BMP4 may contribute to the development of keloid scarring of the skin. SMAD2 is a SMAD family protein that functions as a signal transducer and transcriptional modulator in multiple signaling pathways (26). Gao *et al* demonstrated that silencing SMAD2 with siRNA modulated the synthesis of collagen in keloid-derived fibroblasts (27), and Cohen *et al* suggested that collagen synthesis may suppress keloid scarring (28). CDKN1A is a cyclin-CDK2 complex protein that functions as a regulator of cell cycle

progression at G1 (29), and the accumulation of the cell cycle regulator CDKN1A has been linked to human fibroblast proliferation (30). Therefore, the downregulation of SMAD2 and CDKN1A may promote the progression of keloids. The present study suggests that cell cycle pathway is the significant pathway in keloid-derived fibroblasts tissue. Based on our data, it may be speculated that BMP4, HOXA9, SMAD2 and CDKN1A are suppressors for fibroblasts in keloids and function through the cell cycle pathway.

The results of the present study also indicated that HOXA7 is upregulated, and PSMA4, PSMB2 and CDK1 are downregulated during the development and progression of keloids in keratinocyte tissues. HOXA7 is a transcription factor that is encoded by HOX family genes, and a previous study has revealed abnormal HOX gene expression in normal keratinocytes (31). Hyland *et al* showed that HOXA7 is able to silence differentiation-specific genes in keratinocytes (32). Hence, HOXA7 may be a suppressor for progression in keloid-derived keratinocytes. PSMA4 and PSMB2 are two proteins of the PSM protein family that have key functions in keratinocytes (33). The roles of PSMA4 and PSMB2 in keloid-derived keratinocytes have not been fully defined. However, Amos *et al* suggested that PSMA4 may be associated with susceptibility to keloids (34), and Lim reported that PSMB2 was correlated with keloid therapy exosome (35). The ECM-receptor interaction pathway was found to be a common pathway in the two types of keloid-derived cells. Gene bioinformatics analysis has shown that the ECM-receptor interaction pathway, which is associated with several key genes, is significant in keloids (36). Based on the present results, it is speculated that HOXA7 may be a suppressor while PSMA4 and PSMB2 may contributors in keloid-derived keratinocytes through the ECM-receptor interaction pathway.

In conclusion, the present study identified key genes involved in keloid-derived fibroblasts (BMP4, HOXA9, SMAD2, and CDKN1A) and keratinocytes (HOXA7, PSMA4, and PSMB2) during keloid development and progression through several key pathways such as cell cycle and ECM-receptor interaction pathways. The results may provide a theoretical basis for the mechanistic investigation of keloid scar pathogenesis. However, further studies are required to verify the predicted results.

References

1. Williams FN, Herndon DN and Branski LK: Where we stand with human hypertrophic and keloid scar models. Exp Dermatol 23: 811-812, 2014.
2. Allah K, Yéo S, Kossoko H, Assi Djè Bi Djè V and Richard Kadio M: Keloid scars on black skin: Myth or reality. Ann Chir Plast Esthet 58: 115-122, 2013 (In French).
3. Park TH, Park JH and Chang CH: Clinical features and outcomes of foot keloids treated using complete surgical excision and full thickness skin grafting followed by corticosteroid injections. J Foot Ankle Res 6: 26, 2013.
4. Park TH, Seo SW, Kim JK and Chang CH: Clinical characteristics of facial keloids treated with surgical excision followed by intra- and postoperative intralesional steroid injections. Aesthetic Plast Surg 36: 169-173, 2012.
5. Kelly AP: Medical and surgical therapies for keloids. Dermatol Ther 17: 212-218, 2004.
6. Funayama E, Chodon T, Oyama A and Sugihara T: Keratinocytes promote proliferation and inhibit apoptosis of the underlying fibroblasts: An important role in the pathogenesis of keloid. J Invest Dermatol 121: 1326-1331, 2003.
7. Lim IJ, Phan TT, Song C, Tan WT and Longaker MT: Investigation of the influence of keloid-derived keratinocytes on fibroblast growth and proliferation in vitro. Plast Reconstr Surg 107: 797-808, 2001.
8. Werner S, Krieg T and Smola H: Keratinocyte-fibroblast interactions in wound healing. J Invest Dermatol 127: 998-1008, 2007.
9. Yu H, Bock O, Bayat A, Ferguson MW and Mrowietz U: Decreased expression of inhibitory SMAD6 and SMAD7 in keloid scarring. J Plast Reconstr Aesthet Surg 59: 221-229, 2006.
10. Schmidt M, Schler G, Gruensfelder P and Hoppe F: Expression of bone morphogenetic protein-2 messenger ribonucleic acid in cholesteatoma fibroblasts. Otol Neurotol 23: 267-270, 2002.
11. Hahn JM, Glaser K, McFarland KL, Aronow BJ, Boyce ST and Supp DM: Keloid-derived keratinocytes exhibit an abnormal gene expression profile consistent with a distinct causal role in keloid pathology. Wound Repair Regen 21: 530-544, 2013.
12. Wu Z and Irizarry RA: Preprocessing of oligonucleotide array data. Nat Biotechnol 22: 656-658, 2004.
13. Dennis G Jr, Sherman BT, Hosack DA, Yang J, Gao W, Lane HC and Lempicki RA: DAVID: Database for annotation, visualization and integrated discovery. Genome Biol 4: P3, 2003.
14. Toedling J, Sklyar O, Krueger T, Fischer JJ, Sperling S and Huber W: Ringo - an R/Bioconductor package for analyzing ChIP-chip readouts. BMC Bioinformatics 8: 221, 2007.
15. Storey JD: The positive false discovery rate: A Bayesian interpretation and the q-value. Ann Statist 31: 2013-2035, 2003.
16. Van Rossum G and Drake FL (eds): Python Language Reference Manual. Network Theory Ltd., Godalming, 2011.
17. Wessa P: Pearson correlation (v1.0.6) in Free Statistics Software (v1.1.23-r7). Office for Research Development and Education. URL: http://www wessa net/rwasp_correlation wasp/ 2012.
18. Roux M: Group average linkage compared to Ward's method in hierarchical clustering. In: Visualization and Verbalization of Data. Blasius J and Greenacre M (eds). Chapman and Hall/CRC, Abingdon, pp271-288, 2014.
19. Chatr-Aryamontri A, Breitkreutz BJ, Oughtred R, Boucher L, Heinicke S, Chen D, Stark C, Breitkreutz A, Kolas N, O'Donnell L, *et al*: The BioGRID interaction database: 2015 update. Nucleic Acids Res 43 (Database Issue): D470-D478, 2015.
20. Wang Y and Zheng T: Screening of hub genes and pathways in colorectal cancer with microarray technology. Pathol Oncol Res 20: 611-618, 2014.
21. Smoot ME, Ono K, Ruscheinski J, Wang PL and Ideker T: Cytoscape 2.8: New features for data integration and network visualization. Bioinformatics 27: 431-432, 2011.
22. Eickhoff SB, Schleicher A, Scheperjans F, Palomero-Gallagher N and Zilles K: Analysis of neurotransmitter receptor distribution patterns in the cerebral cortex. Neuroimage 34: 1317-1330, 2007.
23. Rutherford RB, Moalli M, Franceschi RT, Wang D, Gu K and Krebsbach PH: Bone morphogenetic protein-transduced human fibroblasts convert to osteoblasts and form bone in vivo. Tissue Eng 8: 441-452, 2002.
24. Luo S, Benathan M, Raffoul W, Panizzon RG and Egloff DV: Abnormal balance between proliferation and apoptotic cell death in fibroblasts derived from keloid lesions. Plast Reconstr Surg 107: 87-96, 2001.
25. Russell SB, Russell JD, Trupin KM, Gayden AE, Opalenik SR, Nanney LB, Broquist AH, Raju L and Williams SM: Epigenetically altered wound healing in keloid fibroblasts. J Invest Dermatol 130: 2489-2496, 2010.
26. Park JI, Lee MG, Cho K, Park BJ, Chae KS, Byun DS, Ryu BK, Park YK and Chi SG: Transforming growth factor-beta1 activates interleukin-6 expression in prostate cancer cells through the synergistic collaboration of the Smad2, p38-NF-kappaB, JNK, and Ras signaling pathways. Oncogene 22: 4314-4332, 2003.
27. Gao Z, Wang Z, Shi Y, Lin Z, Jiang H, Hou T, Wang Q, Yuan X, Zhao Y, Wu H and Jin Y: Modulation of collagen synthesis in keloid fibroblasts by silencing Smad2 with siRNA. Plast Reconstr Surg 118: 1328-1337, 2006.
28. Cohen I, Keiser H and Sjoerdsma A: Collagen synthesis in human keloid and hypertrophic scar. Plast Reconstr Surg 50: 205, 1972.
29. Pickering MT, Stadler BM and Kowalik TF: miR-17 and miR-20a temper an E2F1-induced G1 checkpoint to regulate cell cycle progression. Oncogene 28: 140-145, 2009.

30. Fournier C, Wiese C and Taucher-Scholz G: Accumulation of the cell cycle regulators TP53 and CDKN1A (p21) in human fibroblasts after exposure to low- and high-LET radiation. Radiat Res 161: 675-684, 2004.
31. Alami Y, Castronovo V, Belotti D, Flagiello D and Clausse N: HOXC5 and HOXC8 expression are selectively turned on in human cervical cancer cells compared to normal keratinocytes. Biochem Biophys Res Commun 257: 738-745, 1999.
32. Hyland PL, McDade SS, McCloskey R, Dickson GJ, Arthur K, McCance DJ and Patel D: Evidence for alteration of EZH2, BMI1, and KDM6A and epigenetic reprogramming in human papillomavirus type 16 E6/E7-expressing keratinocytes. J Virol 85: 10999-11006, 2011.
33. Tan SH, Furusato B, Fang X, He F, Mohamed AA, Griner NB, Sood K, Saxena S, Katta S, Young D, *et al*: Evaluation of ERG responsive proteome in prostate cancer. Prostate 74: 70-89, 2014.
34. Amos CI, Wu X, Broderick P, Gorlov IP, Gu J, Eisen T, Dong Q, Zhang Q, Gu X, Vijayakrishnan J, *et al*: Genome-wide association scan of tag SNPs identifies a susceptibility locus for lung cancer at 15q25.1. Nat Genet 40: 616-622, 2008.
35. Lim SK: Methods of detecting therapeutic exosomes. U.S. Patent No. 20,140,031,256. Filed October 02, 2012; issued January 30, 2014.
36. Huang C, Nie F, Qin Z, Li B and Zhao X: A snapshot of gene expression signatures generated using microarray datasets associated with excessive scarring. Am J Dermatopathol 35: 64-73, 2013.